Available online at www.sciencedirect.com

ScienceDirect

Advances in Space Research 66 (2020) 2302–2318

ADVANCES IN SPACE RESEARCH
(a COSPAR publication)

www.elsevier.com/locate/asr

# Extreme value statistics of wind speed and wave height of the Marmara Sea based on combined radar altimeter data

Berguzar Oztunali Ozbahceci

*Izmir Institute of Technology, Civil Engineering Department, Gulbahce, 35430 Urla, Izmir, Turkey*

Received 1 March 2019; received in revised form 18 August 2019; accepted 20 August 2019
Available online 26 August 2019

**Abstract**

Both reliable and long-term wind and wave data are necessary for the design of coastal and offshore structures. Due to lack of sufficient in-situ measurement data, modeling data have been used in the limited number of wind and wave climate studies of the Marmara Sea. Satellites equipped with instruments capable of observing marine surface wind and ocean waves like Radar Altimeter can be another source for the long term wind and wave climate of the Marmara Sea. In this study, for the first time, the altimeter wind speed and the significant wave height data from different satellite missions are attempted to use in the climate and extreme value analysis of the Marmara Sea. Altimeter wind speeds and significant wave heights are compared with the in-situ measurements and it is found that while the altimeter wind speed agrees with the measurement data, the significant wave height data should be calibrated. After the calibration of the altimeter data and the inter-calibrations of earlier satellite missions, 27 years of altimeter wind speed and wave height data are obtained to use in extreme value analysis. The wind speed and the significant wave height values corresponding to various return periods are determined as a result of extreme value statistics and those values are compared with the results of the measurements and previous studies. Consistent extreme values computed in the current study indicate that the combined radar altimeter data can be used in the wind and the wave climate calculations and the extreme value analysis of the Marmara Sea.


*Keywords:* Radar Altimeter; Significant wave height; Wind speed; Extreme value statistics; Wind and wave climate

## 1. Introduction

The Marmara Sea is an inland sea within the boundaries of Turkey. The Marmara Region including the Marmara Sea connects Europe and Asia through the Bosphorus and Dardanelles Straits. Moreover, Istanbul, the biggest city of Turkey with a population of almost 20 million people is in the Marmara region. Since it is highly developed in industry, commerce, tourism, and transportation, there are many coastal facilities like container terminals, cruise ports, fishery harbors and marinas. Master plan studies show that many types of ports would be necessary in the future along the coasts of the Marmara Sea (Ministry of Transport, 2010).

Reliable wind and wave data affecting a coastal region is very essential for almost all coastal and marine activities. Especially for the design of the coastal structures, not only reliable but also long-term data are necessary. Although in-situ measurements produce the most reliable source of wind and wave data, due to the practical and financial problems associated with these measurements, short term measurement campaigns have been organized in the Marmara Sea. In 2013, the State Meterological Organisation of Turkey started to permanent offshore wind and wave measurements in Silivri and Adalar at the North and East of the Marmara Sea, respectively. Since the data have been collected almost for 5 years, they are not suitable to use in

*E-mail address:* berguzarozbahceci@iyte.edu.tr

https://doi.org/10.1016/j.asr.2019.08.025
0273-1177/

climate analysis. However, they can be used for the calibration and verification purposes.

Due to lack of sufficient in-situ measurement data, modeling data have been used in the limited number of climate studies of the Marmara Sea. The Wind and Deep Water Wave Atlas prepared within the framework of NATO-TU-WAVES project by Ozhan and Abdalla (2002) has become an important data source not only for the Marmara Sea but also for all Turkish coasts. Nearly 8 years (1991–1998) of wind fields data produced by ECMWF (The European Centre for Medium-Range Weather Forecasts) were used to compute long-term wind and wave statistics. To compute extreme value statistics, synoptic maps corresponding to the selected major (extreme) storms were digitized. Then, the wind fields were produced from those digitized synoptic maps by using the gradient wind model of Lavrenov (Abdalla and Ozhan, 1999). Although both set of the wind fields are reliable enough for large basins like the Black Sea and the Mediterranean, it was recognized that they are not proper for the Marmara Sea (Ozhan and Abdalla, 1999). A wind model based on atmospheric pressure records of the meteorological stations surrounding the Marmara Sea basin was developed by Erkal (1997) and modified by Abdalla and Ozhan (1998). Then long term and extreme wind and wave data for the Marmara Sea were presented in a printed Atlas. After this Atlas, wave climate of the Marmara Sea was investigated in three more studies. Saracoğlu (2011) and Abdollahzadehmoradi et al. (2014) obtained the wind and deep water wave climate for the Marmara Sea using the wind fields from ECMWF and the 3rd generation wave model Mike 21 SW. Kutupoglu et al. (2018) used CFSR winds from the NOAA/NCEP and a high-resolution SWAN wind wave hindcast model. The comparison study of Saracoğlu (2011) shows that his wave results for the Marmara Sea do not coincide with those of Ozhan and Abdalla (2002). In fact, it is stated that the Atlas overpredicts the extreme waves of the Marmara Sea. Saracoğlu (2011) estimates the maximum significant wave height (SWH) in Marmara Sea with a 50-year return period as 4 m. Kutupoglu et al. (2018) recommend to use the calibrated SWAN model forced by CFSR winds for the Marmara Sea. Moreover, extreme wave height values are estimated to be around 3 m for a 100-year return period.

Satellites that are equipped with instruments capable of observing marine surface wind and ocean waves like Radar Altimeter (RA), Synthetic Aperture Radar (SAR) and Scatterometer provide valuable data. Such data sources have good global coverage and are usually very reliable (Abdalla, 2013). Janssen et al. (2007) and Abdalla et al. (2011) showed through a triple collocation technique, that at the scale of the model (around 75 km) the error of SWH is almost 6% of mean SWH, while the error in wind speed is 1.0 m/s. The duration of data that can be obtained from most of the satellites is less than 15 years due to the lifetime of the satellites. However, it is possible to extend the duration of the measured data by combining measurements from different satellites. When using measurements from different satellites, an inter-calibration of the instruments is required. Zieger et al. (2009) combined wind speed and significant wave height data from seven altimeter missions to obtain consistent data for a period of more than 23 years. Vinoth and Young (2011) used the 23 years consistent altimeter data to determine extreme values of wind speed and SWH corresponding to a 100-yr return period. They used both the initial distribution method (IDM) and peaks-over-threshold (POT) approaches for extreme value computations and concluded that the satellite altimeter can provide high quality estimates of extreme wind speed and wave height conditions on a global basis. Hithin et al. (2015) used and combined altimeter data from seven missions for the period 1996–2012 to investigate the trends of wave height and period in the Central Arabian Sea.

Satellite altimeter data can be another source to derive long term wind and wave climate of the Marmara Sea, in which a limited number of studies have been undertaken. In this study, for the first time, the altimeter wind speed ($u_{10}$) and SWH data from different missions are used in the climate and extreme value analysis of the Marmara Sea. Section 2 provides an overview of the satellite and in-situ measurement data of the State Meteorological Organization of Turkey used in the study. The comparison between the altimeter and in-situ measurement data is provided in Section 3. Extension and the inter-calibration study of radar altimeter data are given in Section 4. Section 5 presents the extreme value analysis of the significant wave height and the wind speed. Finally, conclusions are presented in Section 6.

## 2. Overview of data used

### 2.1. In-situ measurement data

There are two offshore measurement stations in Marmara Sea. The locations of the stations are presented in Fig. 1. One of them is Silivri buoy station located at 40.9742° N and 28.2487° E. The offshore station is at 4 km away from the coast of Silivri, one of the districts of Istanbul.

Deployment depth of the buoy is 50 m. It is shown in Fig. 2. It is a SEAWATCH Midi 185 Buoy equipped with an ultrasonic anemometer as it is seen in Fig. 2 (ONHO, 2015). The accuracy of the measured wind speed by the anemometer is given as 2% at 12 m/s. The buoy measures wind speed at 3 m above the sea surface. Therefore measured wind data is converted to the wind speed at 10 m above the sea surface, $U_{10}$ using Hellman formula $U_{10} = U_z^*(10/z)^{1/7}$ with $z = 3$ m (personal communication with Turkish state of Meteorological Services). Hourly averaged wind speeds and the directions are given as output. Wind measurements began on May 7th, 2013. The total number of wind data available for a period of almost five years is 27430. A brief summary of the wind measure-

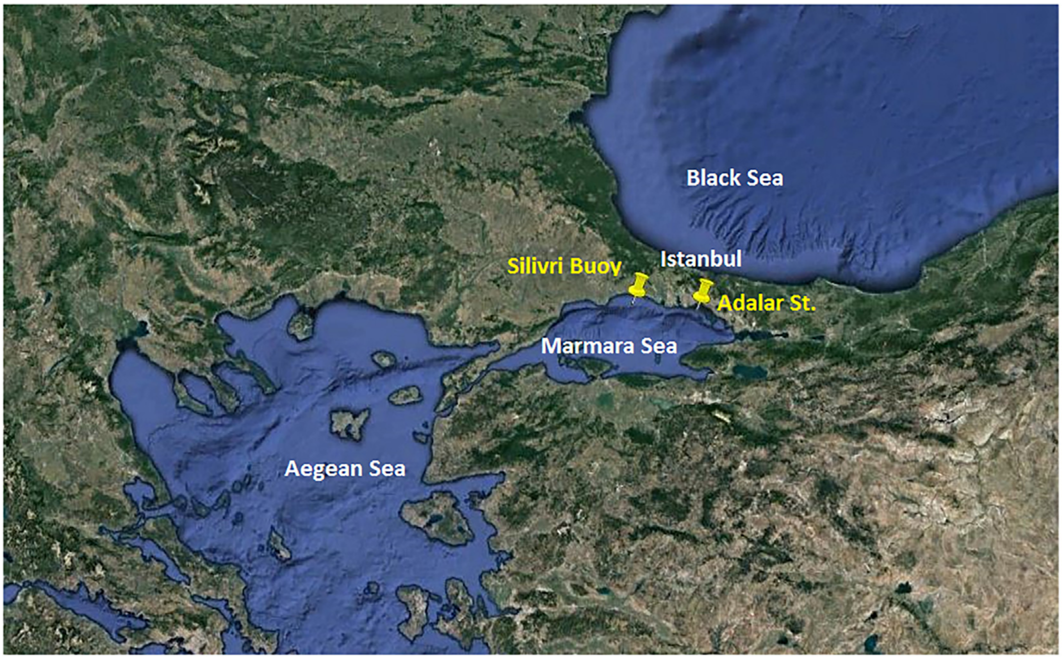


Fig. 1. Locations of the measurement stations.

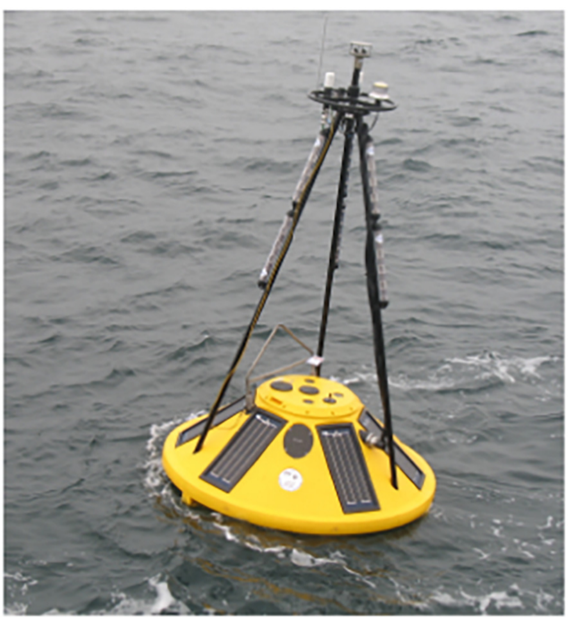

Fig. 2. Silivri Buoy Station (https://www.mgm.gov.tr/deniz/deniz-omgi.aspx).

ment periods is given in Table 1. Table 1 shows that there are almost no data collected in 2016 and 2017 due to various reasons. If the measurement duration is more than half of the month, it is represented by "✔" in Table 1.

Silivri buoy measures the waves by waveSense 3 sensor (ONHO, 2015). It is an inertial motion sensor using accelerometers, angular rate sensors, magnetoresistive sensors and temperature sensor for compensating temperature effects (https://www.fugro.com/about-fugro/our-expertise/technology/seawatch-metocean-buoys-and-sensors). Accuracy of the sensor is given as $\pm$ 10 cm. Time series of 3-dimensional buoy motion and wave parameters like height, period, direction and a number of other parameters are the outputs of the sensor. Wave measurements were also begun on May 7th, 2013. The total number of hourly wave data available for a period of almost five years is 36813. Wave measurement durations are given in Fig. 3.

The other offshore measurement station in Marmara Sea is Adalar station as shown in Fig. 4. It is located at 40.9328° N and 28.9489° E. The location is shown in Fig. 1. The offshore station is close to the islands of Istanbul. It is located 8 km from Kinali island, 8 km from the Kadikoy coast and 7 km from the Zeytinburnu coast. Only the wind has been measured in Adalar station. Measured wind speed data by a sensor at 2 m above the sea surface converted to $U_{10}$ wind speed using the Hellman formula as it is in the case of Silivri station. Wind speed measurements were started in 01st of May 2013. The total number of wind speed data available for a period of almost five years is 26117. Brief summary of the measurement durations is given in Table 2. If the measurement period is more than the half of the month, it is represented by "✔" in Table 2.

### 2.2. Altimeter data

To compare the altimeter and in-situ measurement data, ideally, it is desirable to collocate the altimeter and buoy observations at no spatial or temporal difference (Abdalla et al., 2011). However, then, it would be possible to find only very few collocations. Therefore a matchup area shown in Fig. 5 was selected such that Silivri buoy and

Table 1
Brief summary of wind measurement periods in Silivri Station.

| | Months | | | | | | | | | | | |
|---|---|---|---|---|---|---|---|---|---|---|---|---|
| years | J | F | M | A | M | J | J | A | S | O | N | D |
| 2013 | | | | | ✓ | ✓ | ✓ | ✓ | ✓ | ✓ | ✓ | ✓ |
| 2014 | ✓ | ✓ | ✓ | ✓ | ✓ | ✓ | ✓ | ✓ | ✓ | ✓ | ✓ | ✓ |
| 2015 | ✓ | ✓ | ✓ | ✓ | ✓ | ✓ | ✓ | ✓ | ✓ | ✓ | ✓ | ✓ |
| 2016 | ✓ | X | X | X | X | X | X | X | X | X | X | X |
| 2017 | X | X | X | X | X | X | X | X | X | X | X | X |
| 2018 | X | X | ✓ | ✓ | ✓ | ✓ | | | | | | |

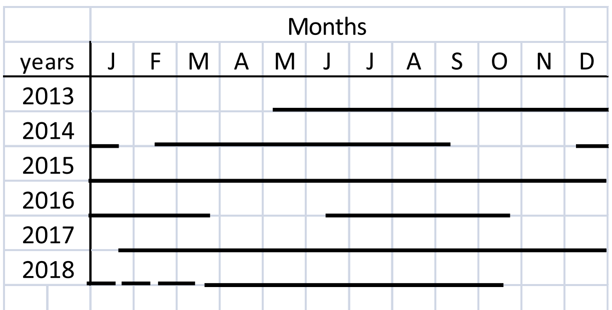


Fig. 3. Wave measurement durations in Silivri Station.

Fig. 4. Adalar offshore Station (https://www.mgm.gov.tr/deniz/deniz-omgi.aspx).

satellite data separated by no more than 0.5 deg in latitude/longitude as recommended by Young et al. (2011). The same matchup area was used for the comparison between the satellite data and Adalar station. The matchup time is also important and it was determined as 30 min. All the satellite missions data in the defined matchup area was retrieved from the RADS (Radar Altimeter Database System) developed first at Delft University of Technology (Scharroo et al., 2013). The missions with the available data are ERS-1, ERS-2, Envisat, TOPEX, Poseidon, Jason1, Jason2, Jason3, CryoSat2, Saral and Sentinel3. The durations of these satellite missions are given in Fig. 6. Detailed information about the repeat cycle, altitude, inclination of these satellites can be found in Zieger et al. (2009), Abdalla (2013) and Hithin et al. (2015).

## 3. Comparison study

### *3.1. Wind speed ($u_{10}$)*

Since the radar altimeter (RA) provides data along a linear track, there are a number of RA data matching a buoy data in a particular time. In this study, those collocated RA data are simply averaged for the comparison. Jason2, Saral, CryoSat2, Jason3 and Sentinel3 are the satellite missions with available wind speed data for the measurement periods of in-situ data given in Table 1. Tracks of these satellites within the matchup area are given in Fig. 7. Firstly, altimeter $u_{10}$ data from all satellites are individually compared with the Silivri buoy data for the period 2013–2018. Comparison plots of the altimeter data with the Silivri buoy data are given in Fig. 8. Plots of the satellites Jason3 and Sentinel3 are not given because the collocation numbers are less than 30 for these satellites. The reason for

Table 2
Brief summary of wind measurement periods in Adalar Station.

| | Months | | | | | | | | | | | |
|---|---|---|---|---|---|---|---|---|---|---|---|---|
| years | J | F | M | A | M | J | J | A | S | O | N | D |
| 2013 | | | | | ✓ | ✓ | ✓ | ✓ | ✓ | X | ✓ | X |
| 2014 | X | X | X | X | ✓ | ✓ | ✓ | X | X | X | ✓ | ✓ |
| 2015 | ✓ | ✓ | X | ✓ | ✓ | ✓ | ✓ | ✓ | ✓ | ✓ | ✓ | ✓ |
| 2016 | ✓ | ✓ | ✓ | ✓ | ✓ | ✓ | ✓ | ✓ | ✓ | ✓ | ✓ | ✓ |
| 2017 | ✓ | ✓ | ✓ | ✓ | ✓ | X | X | X | X | X | X | X |
| 2018 | X | X | ✓ | ✓ | ✓ | ✓ | | | | | | |

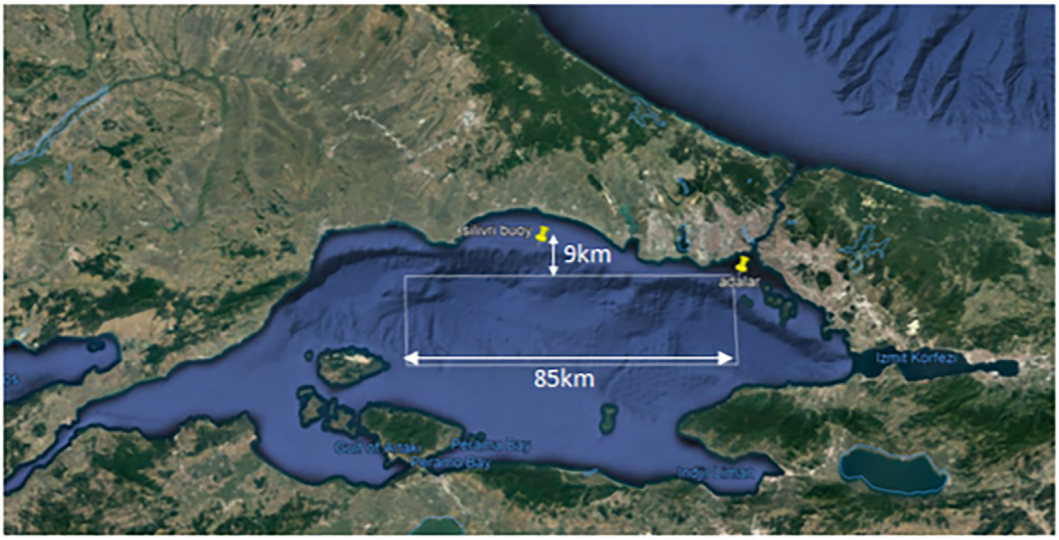


Fig. 5. Measurement stations and the selected matchup area to collocate the RA and the in-situ data.

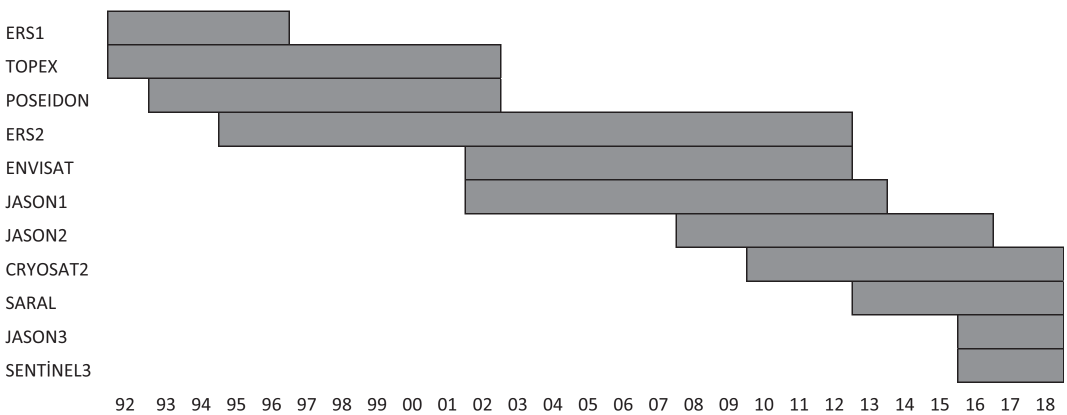


Fig. 6. The durations of the satellite missions with the available data for the matchup in the Marmara Sea.

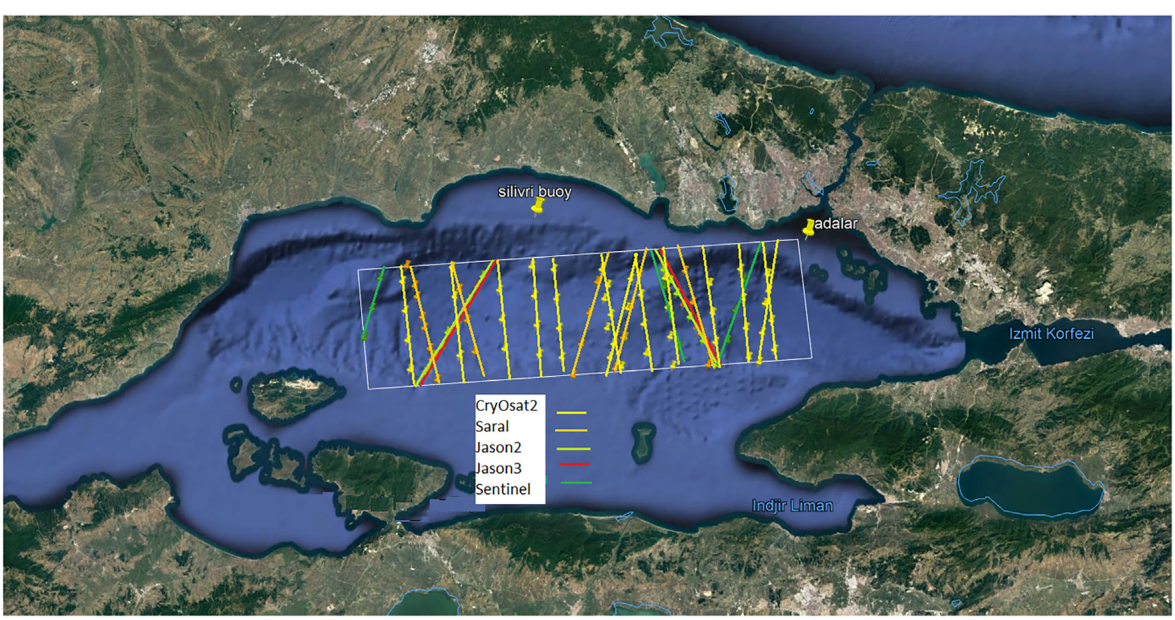


Fig. 7. Tracks of Jason2, Saral, CryoSat2, Jason3 and Sentinel3 within the matchup area.

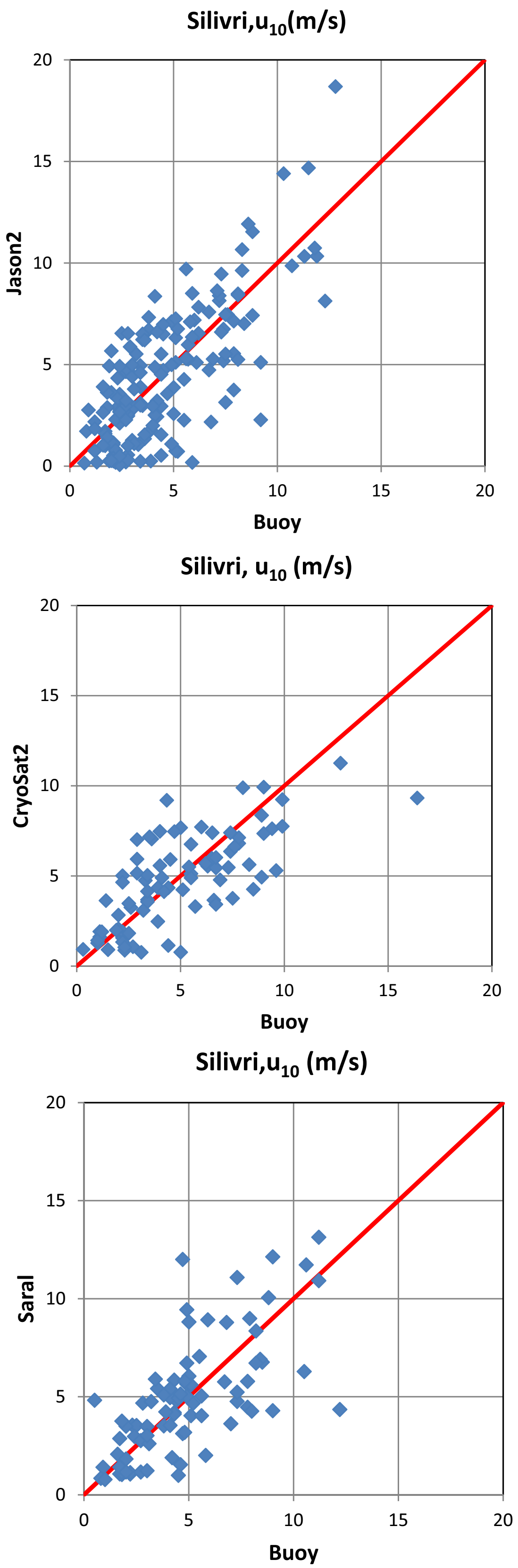


Fig. 8. Scatter plots of the altimeter data (Jason2, CryoSat2 and Saral) and the Silivri buoy data.

the insufficient data is that there is not buoy data for most of 2016 and 2017 as can be seen in Table 1. Fig. 8 shows that three of the satellites' wind speed data agree with the buoy data, although they are scattered.

For the error assessment, RMSE (Root Mean Square Error), SI (Scattered Index), Bias, symmetric slope, A ($y = Ax$) and the correlation coefficient, R, are calculated and the results are presented together with the data numbers and the mean values of altimeter and buoy wind speeds in Table 3. Since the collocation numbers (28 and 17 collocations for Jason3 and Sentinel3, respectively) are not sufficient for a statistical analysis, error assessments of Sentinel3 and Jason3 are not given in Table 3. In order to increase the collocation number, all the altimeter data (Jason2, CryoSat2, Saral, Jason3, Sentinel3) are combined by aggregation simply and one satellite database is obtained. If RA data of different missions are coinciding, average of them is collocated with the buoy data. Therefore the number of combined data may be less than the addition of the numbers of each RA data. The error assessment of the combined altimeter data is also presented in the last row of Table 3. As can be seen in Table 3, there is a slight increase in the error in case of combined altimeters.

The RMSE of altimeter measurements for wind speed in Table 3 is slightly higher than the 1.0–2.0 m/s range given in the previous studies (Zieger et al., 2009, Abdalla et al., 2011, Hithin et al., 2015). However, it should be noted here that the Marmara Sea is a small inland sea where the effect of 'land contamination' on the quality of the satellite data is unavoidable.

Kutupoglu et al. (2018) compared ERA-Interim reanalysis wind speed data with the Silivri buoy wind speed data. They concluded that the ERA-Interim winds showed lower estimates over the measurements. In this study ERA5, the new re-analysis data of ECMWF is compared to Silivri buoy data to check the error of altimeter data. ERA5 which will eventually replace the ERA-Interim reanalysis provides hourly estimates of a large number of atmospheric, land and oceanic climate variables. The data cover the Earth on a 30 km grid and resolve the atmosphere using 137 levels from the surface up to a height of 80 km (https://www.ecmwf.int/en/forecasts/datasets/archive-datasets/reanalysis-datasets/era5). Since it is possible to match ERA5 data for each hourly measured buoy data, the collocation number is 23427. While the comparison plot is given in Fig. 9, the error assessment of ERA5 is presented in Table 4. Fig. 9 and Table 4 show that RMSE is lower in ERA 5 than in the altimeter and ERA5 is less scattered. However, it seems that wind speed is underestimated by ERA5.

Considering that the purpose of the study is to compute extreme value statistics of the wind speed and the significant wave height, an agreement between the altimeter and the buoy data in terms of probability distributions may be more significant than agreement in terms of time

Table 3
Error assessment for the wind speed of different satellites and combination of them against Silivri Buoy.

| Satellite | Data no | Mean RA | Mean buoy | RMSE | SI | Bias | A | R |
|---|---|---|---|---|---|---|---|---|
| Jason2 | 164 | 4.3625 | 4.5280 | 2.186453 | 0.482869 | −0.1655 | 0.956799 | 0.75156 |
| CryoSat2 | 83 | 4.8079 | 4.9994 | 2.118906 | 0.423832 | −0.19146 | 0.872358 | 0.711923 |
| Saral | 86 | 4.8490 | 4.8558 | 2.208478 | 0.454811 | −0.00682 | 0.942289 | 0.685435 |
| Combined | 373 | 4.3679 | 4.8507 | 2.402666 | 0.495326 | −0.48274 | 0.855639 | 0.664085 |

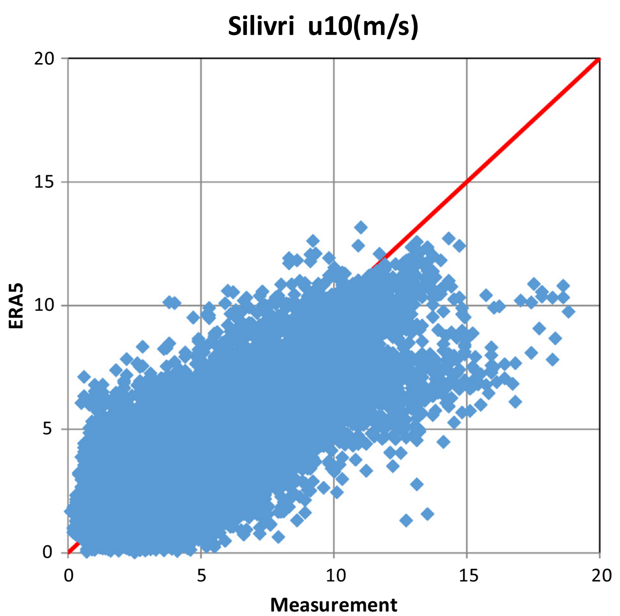


Fig. 9. Wind speed comparison between ERA5 and the Silivri buoy.

series and scatter plots. In this study, Quantile-Quantile plots (Q-Q plots) are used to compare the probability distributions of the altimeter data and the in-situ measurement data by plotting their quantiles against each other. In order to calculate the quantiles, all the data of the altimeter and the buoy collected in the same time period are used without considering whether they are collocated in time or not. For example, the altimeter data recorded in 2017 are not included in the quantile calculations since there is no buoy measurement in 2017. Similarly, since Jason2 has no data after 2016, the buoy data collected in 2018 are not considered during the quantile calculations of the Jason2 and the buoy. Q-Q plots of Silivri buoy data versus Jason2, CryoSat2, Saral and the combined altimeter data are shown in Fig. 10. While the individual altimeters underestimate or overestimate the probability of high wind speeds, the combination of the altimeters results a good agreement with the buoy as can be seen in Fig. 10.

The same altimeter data are also compared with the wind measurements in Adalar station. An error assessment for the wind speed, u10, of different satellites and combination of them against Adalar station measurement is given in Table 5.

Table 5 indicates that the error increases when the altimeter wind speed data is compared with in-situ measurement in Adalar station. The reason may be the higher spatial difference between the RA and in-situ measures for Adalar station compared to Silivri station.

A similar quantile–quantile analysis was carried out for $u_{10}$ to compare the combination of Jason2, CryoSat2, Saral, Jason3 and Sentinel3 altimeters and the in-situ measurements in Adalar station. Q-Q plot is shown in Fig. 11.

Fig. 11 shows that the combined altimeters are capable of catching high wind speeds of Adalar station although the agreement between the RA and the in-situ data is not good as the Silivri case. Therefore it can be concluded from the comparison study that the satellite RA data can be used for the extreme wind analysis of the Marmara Sea.

### 3.2. Significant wave height (SWH)

After the wind speed comparison was completed, a similar comparison study was carried out for the significant wave height. The SWH data of the five satellites, Jason2, CryoSat2, Saral, Jason3 and Sentinel3 recorded within the matchup area given in Fig. 5 were collocated with the Silivri buoy data measured between 2013 and 2018. Comparison plots for SWH of Silivri buoy versus individual satellites and the combination of them are given in Fig. 12. Fig. 12 shows that the agreement between RA data and the buoy data is not so good. Altimeters measure higher SWH compared to the Silivri buoy. Statistical error parameters for the SWH of individual and combined altimeters against the buoy measurements are given in Table 6. The error parameters for the combination of five satellites are also presented in the last row of Table 6.

As can be seen in Table 6, the bias, RMSE and SI values are high compared to the previous comparison studies (Hithin et al., 2015, Abdalla and Yılmaz, 2015). The reason may be the effect of unavoidable 'land contamination' for a small inland sea on the quality of the satellite data. The difference between the RA and the buoy measurements of SWH may also be due to spatial differences between the measurements. Quantile-Quantile analyses also show the overes-

Table 4
Error assessment for the wind speed of ERA5 against Silivri Buoy.

| Data no | Mean ERA5 | Mean buoy | RMSE | SI | Bias | A | R |
|---|---|---|---|---|---|---|---|
| 23,427 | 4.0310 | 4.7678 | 1.8587 | 0.3899 | −0.7368 | 0.7878 | 0.7819 |

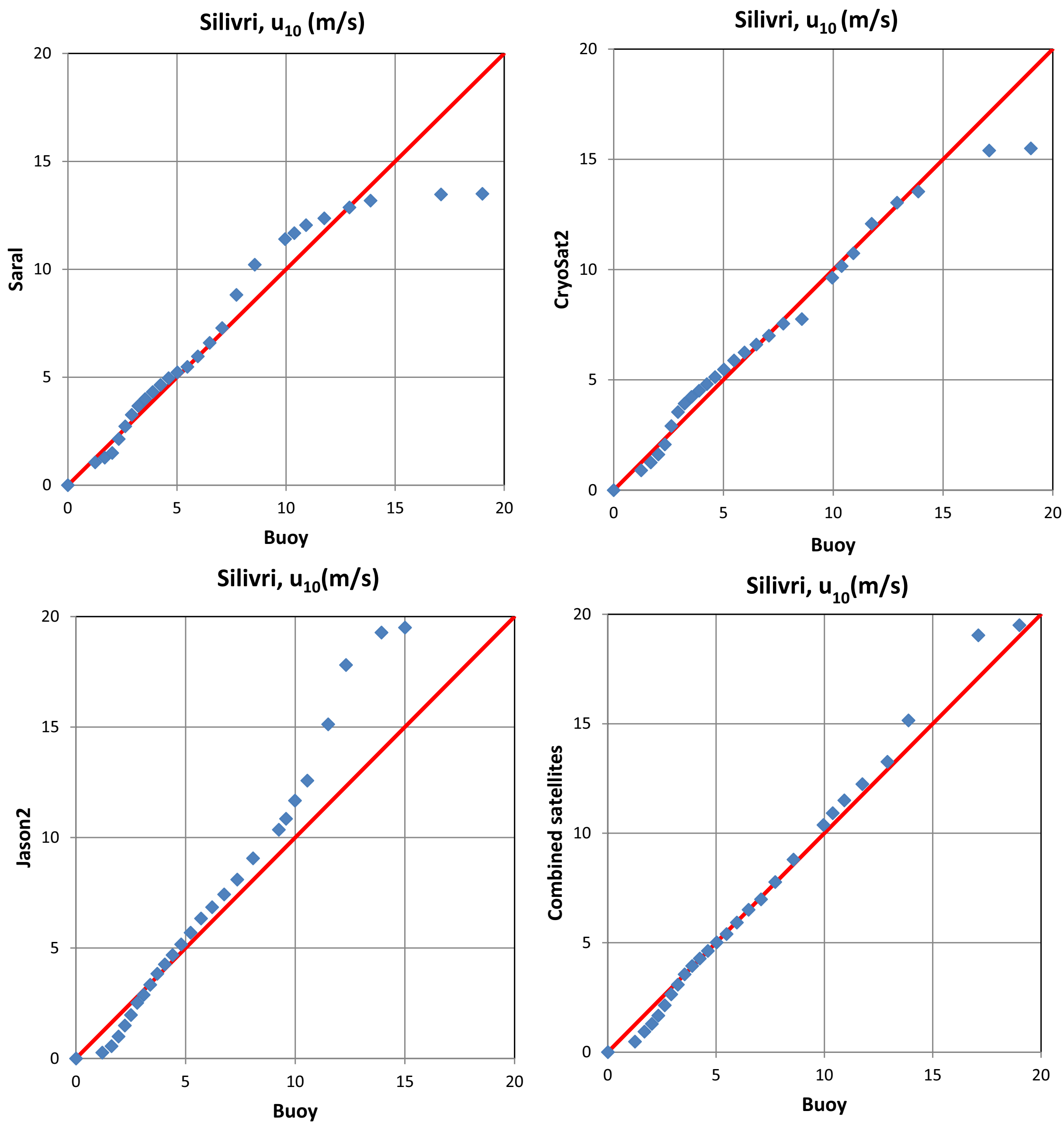


Fig. 10. Q-Q plots of Silivri buoy data versus Jason2, CryoSat2, Saral and the combined altimeter data.

Table 5
Error assessment for the wind speed, $u_{10}$, of different satellites and combination of them against Adalar station measurement.

| Satellite | Data no | Mean RA | Mean buoy | RMSE | SI | Bias | A | R |
|---|---|---|---|---|---|---|---|---|
| Jason2 | 158 | 4.4203 | 5.8038 | 2.6703 | 0.4601 | −1.3835 | 0.7499 | 0.7145 |
| CryoSat2 | 96 | 4.8825 | 6.0667 | 2.2549 | 0.3717 | −1.1842 | 0.7803 | 0.7744 |
| Saral | 102 | 4.6601 | 5.5598 | 2.1157 | 0.3805 | −0.8997 | 0.8160 | 0.7419 |
| Jason3 | 103 | 4.1741 | 5.5301 | 2.5846 | 0.4674 | −1.3560 | 0.7220 | 0.6960 |
| Combined | 466 | 4.4798 | 5.6929 | 2.4559 | 0.4314 | −1.2131 | 0.7667 | 0.7286 |

timation of the satellite data. The Q-Q plot for the SWH of the combined satellites versus Silivri buoy is given in Fig. 13.

Fig. 13 shows that the combined satellite is capable of catching the highest SWH. However it overestimates the rest of the data. It means that a calibration is necessary to use the radar altimeter data in the long-term and extreme value statistics of the significant wave height in the Marmara Sea.

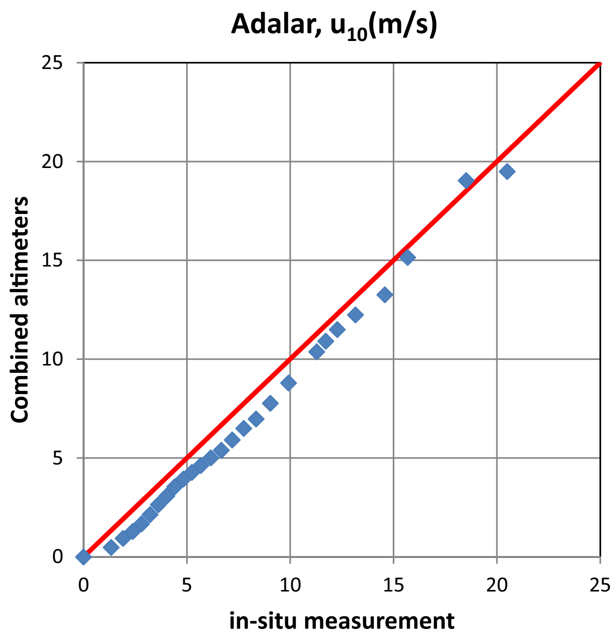


Fig. 11. Q-Q plot for the wind speed of in-situ measurement in Adalar station against the combined altimeters.

## 4. Extension of the altimeter data to be used in the extreme value statistics

Satellites used in the comparison study given in Section 3 have no measurement before 2008. It means that there are ten years of altimeter data and they may not be enough to compute the extreme values statistics. Fig. 6 shows that there are some earlier altimeter data. Therefore the recent altimeter data should be combined with the earlier satellite data. Combining measurements can extend the duration of the continuous altimeter time record to more than two decades. However, the characteristics of the measurements of various altimeters may be different. Therefore, any attempt to carry out climate computations from a combination of radar altimeters must include an inter-calibration exercise (Abdalla, 2013).

Among the five satellites: Jason2, Saral, CryoSat2, Jason3 and Sentinel3, only Jason2 has collocations with the earlier satellites Jason1 and Topex. Overlapped time periods of three satellites are demonstrated in Fig. 6.

### 4.1. Wind Speed, $u_{10}$

In order to inter-calibrate the Jason2, Jason1 and Topex measurements, the data in the overlapped time of two satellites are extracted and compared. The number of collocating wind speed data is 242 for Jason2 and Jason1 and 191 for Jason1 and Topex. The comparison is done with Q-Q analysis. Q-Q plots for the wind speed of Jason2 versus Jason1 and Jason1 versus Topex are shown in Fig. 14. As can be seen in Fig. 14, there is a perfect agreement for the wind speed of Jason2 and Jason1 RA. Jason1 and Topex also agree well. However, a correction is necessary for higher winds.

Inter-calibrated Jason family RA wind speed data are combined with the data of recent satellites of Saral, CryoSat2, Jason3 and Sentinel3 in order to extend the duration of combined satellite data. As a result, 27 years wind speed data are obtained.

### 4.2. Significant wave Height, SWH

In Section 3.2, SWH of combined altimeter is compared with that of Silivri buoy, and it is concluded that a calibration is necessary to use the radar altimeter data in the computation of extreme SWH statistics for the Marmara Sea. Since the Jason family satellites, Jason2, Jason1 and Topex should be inter-calibrated, firstly Jason2 is calibrated with Silivri Buoy data. Fig. 15 shows the Q-Q plots for SWH of Silivri Buoy versus Jason2 before calibration and after calibration.

As can be seen in top plot of Fig. 15, Jason2 overestimates the SWH. However it catches the highest wave. Therefore Jason2 is calibrated if the SWH is less than 2.7 m. Quadratic regression function is used in the calibration with the square of correlation coefficient, $R^2 = 0.9968$. Fig. 15 also shows that Jason2 SWH agrees with the buoy SWH after calibration.

After SWH of Jason2 is calibrated, an inter-calibration study similar to that performed for the wind speed is carried out for the SWH. The number of collocating data is 115 for Jason2 and Jason1 and 116 for Jason1 and Topex. The comparison is performed in terms of Q-Q analysis. Q-Q plots for SWH of Jason2 versus Jason1 and Jason1 versus Topex are shown in Fig. 16. Fig. 16 indicates that Jason2 and Jason1 as well as Jason1 and Topex agree well.

After inter-calibration, Jason family altimeters are calibrated with respect to the buoy measurements using Fig. 15. Then, they are combined with the recent data of satellites of Saral, CryoSat2, Jason3 and Sentinel3 in order to extend the duration of combined satellite data. As a result, 27 years of the significant wave height data are obtained.

## 5. Extreme value statistics

The purpose of the extreme value computation is to estimate an expected value of an extreme event which may occur once in a long period of time. This long period of time is named the return period (Rp). Extreme value analysis starts with the computation of the cumulative distribution of the data which is to be fitted to a distribution function. Fitting to a distribution function is necessary to extrapolate the data set to the extreme values corresponding to longer return periods with lower probabilities (Kamphius, 2000). Then the best fitting distribution is examined since the parent distribution is mostly unknown.

The ordered data are used specifically for the analysis of extreme values. The maximum annual data or the data cho-

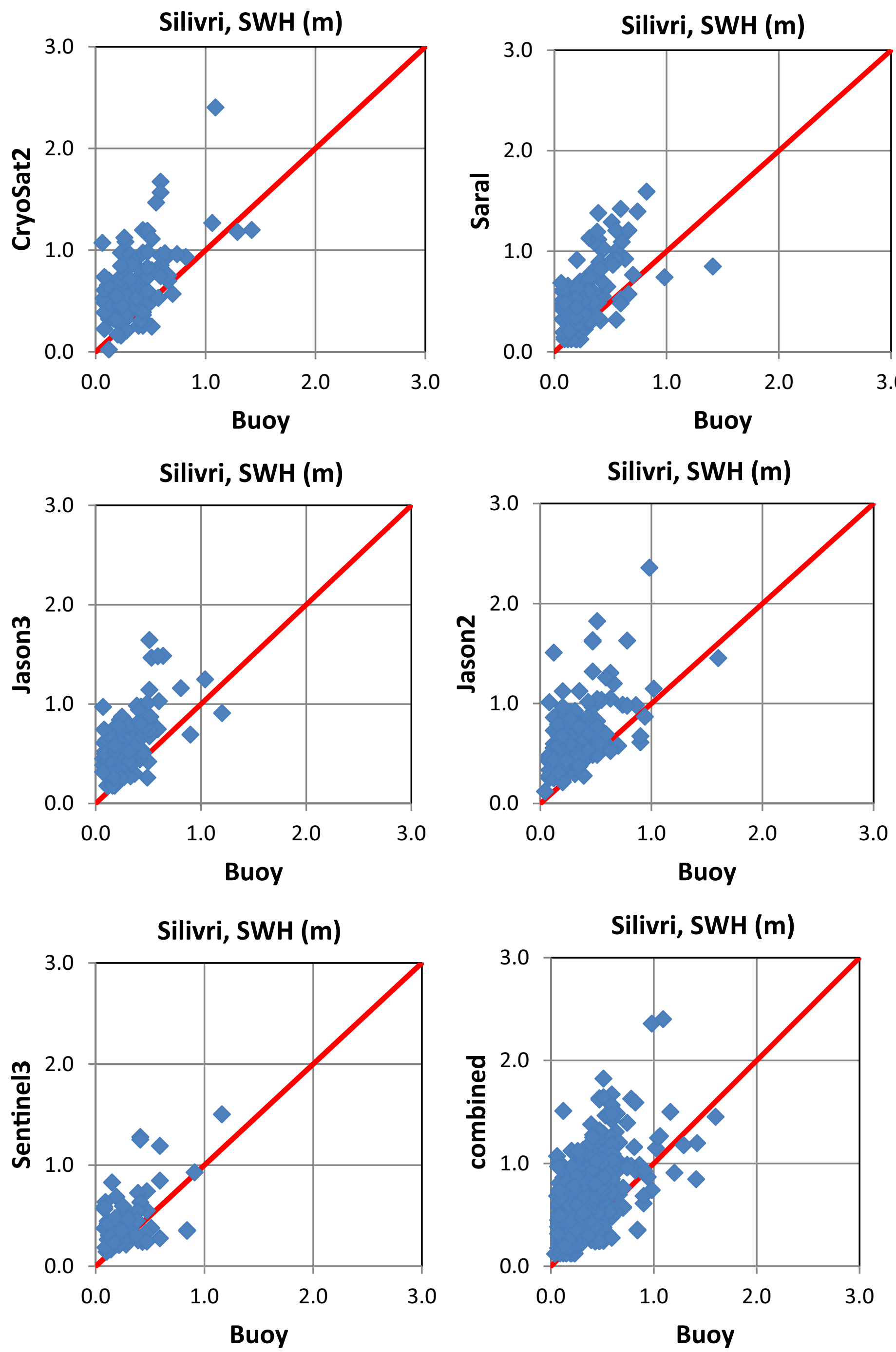


Fig. 12. Comparison plots for SWH of individual RA and the combination of them.

Table 6
Statistical error parameters for the SWH of RA against the Silivri buoy.

| Satellite | Data no | Mean RA | Mean buoy | RMSE | SI | Bias | A | R |
|---|---|---|---|---|---|---|---|---|
| Jason2 | 178 | 0.6332 | 0.3244 | 0.4123 | 1.2712 | 0.3088 | 1.5929 | 0.5541 |
| CryoSat2 | 104 | 0.6713 | 0.3663 | 0.4229 | 1.1544 | 0.3050 | 1.5329 | 0.5769 |
| Saral | 131 | 0.5438 | 0.2936 | 0.3550 | 1.2091 | 0.2502 | 0.9520 | 0.6041 |
| Jason3 | 131 | 0.5680 | 0.2892 | 0.3573 | 1.2358 | 0.2788 | 1.6434 | 0.5971 |
| Sentinel3 | 77 | 0.4459 | 0.2929 | 0.2795 | 0.9546 | 0.1531 | 1.2456 | 0.5177 |
| Combined | 603 | 0.5855 | 0.3131 | 0.3799 | 1.2134 | 0.2724 | 1.5510 | 0.5763 |

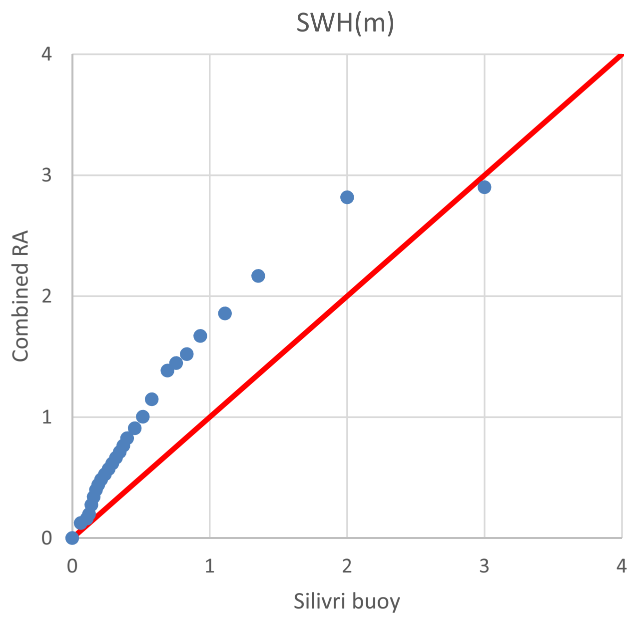


Fig. 13. Q-Q plot for SWH of Silivri Buoy versus the combined altimeters.

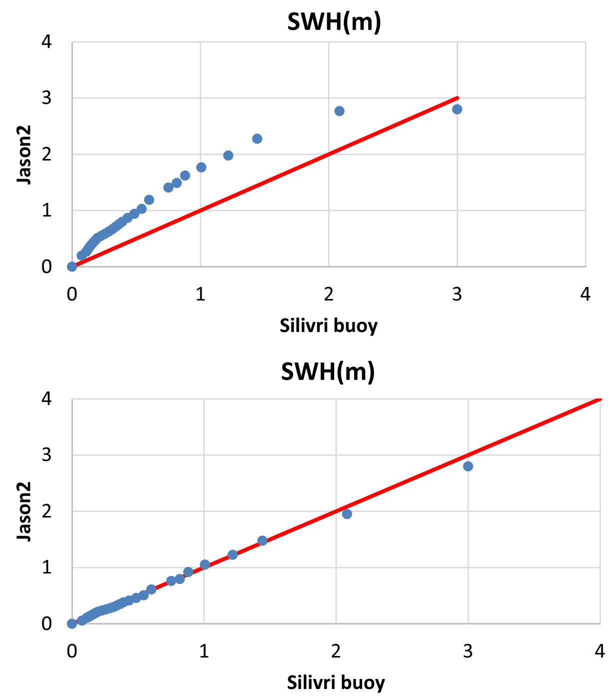


Fig. 15. Q-Q plots for SWH of Silivri Buoy versus Jason2 before calibration (at the top) and after calibration.

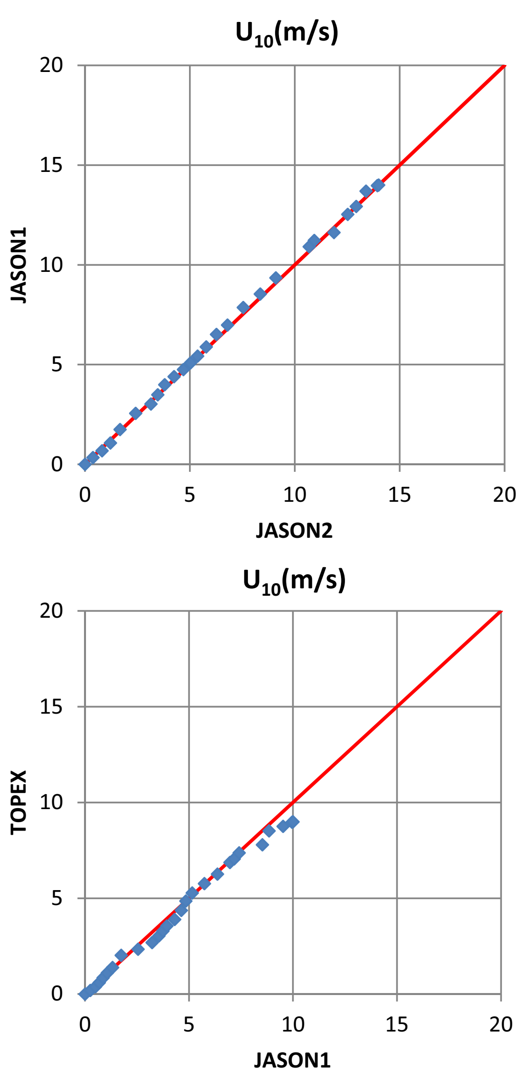


Fig. 14. Q-Q plots for the wind speed of Jason2 versus Jason1 (above) and Jason1 versus Topex (below).

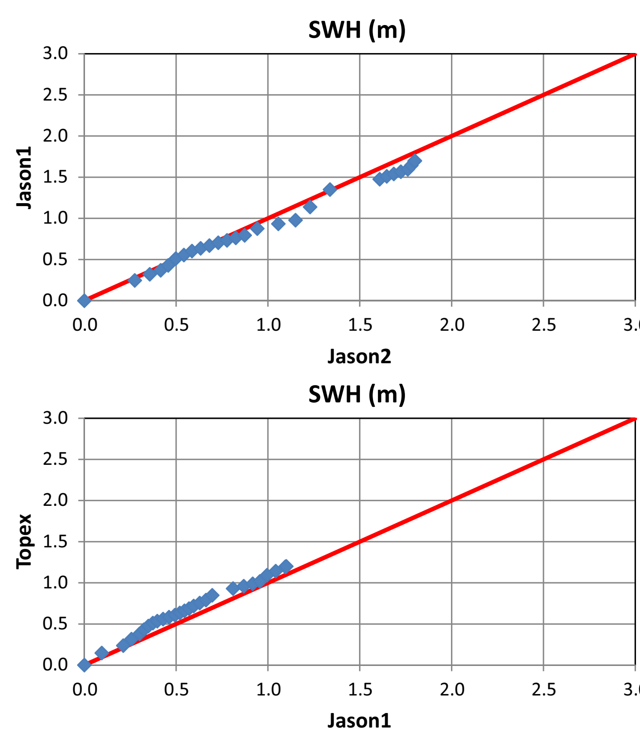


Fig. 16. Q-Q plots for the SWH of Jason2 versus Jason1 and Jason1 versus Topex.

sen by peak over threshold (POT) method are used. In this study annual maxima of 27 years of data are used. They are arranged in descending order and non-exceedance probabilities are calculated from ordered samples by using plotting position formula. The best-known formula to calculate the non-exceedance probability is the modified Weibull formula given in Eq. (1) (Goda, 2010).

$$P(x) = \frac{m - \alpha}{N + \beta} \tag{1}$$

where; P (x) is the probability of non-exceedance, m = order number, N = data number, α and b are the coefficients changing according to the used theoretical distribution function.

The cumulative distribution functions of the commonly used distributions are given below (Goda, 2010):

Fisher Tippet I (Gumbel)

$$P(x) = exp\left[-\exp(-\frac{x - B}{A})\right] : \quad -\infty < x < \infty \tag{2}$$

Fisher Tippet II

$$P(x) = exp\left[-(1 + \frac{x - B}{kA})^{-k}\right] : \quad B - kA < x < \infty \tag{3}$$

Weibull

$$P(x) = 1 - exp\left[-(\frac{x - B}{A})^{k}\right] : \quad B \ll x < \infty \tag{4}$$

Log-normal,

$$P(x) = \int_{-\infty}^{x} p(t)dt : \quad 0 < x < \infty$$

$$p(x) = \frac{1}{\sqrt{2\pi}Ax} exp\left[-\frac{(lnx - B)^2}{2A^2})\right] \tag{5}$$

where; A ,B and k are the scale, the location and the shape parameters, respectively.

Fitting a distribution function to the calculated non-exceedance probabilities of the sample data is performed by obtaining the A, B and k parameters. There are different methods to obtain those parameters like the least square method, the method of moments and the maximum likelihood method. In this study, the least squares method was used. Gumbel, Log-normal, Fisher Tippet II (k = 2.5, 3.33, 5.0 and 10.0) and Weibull (k = 0.75, 1.0, 1.4, and 2.0) distributions were used as the candidate distributions to examine the best fitting distribution function. Then the goodness of fit is tested by using the square of correlation coefficient, MIR Criterion (MInimum Ratio of residual cor. coeff.) , DOL criterion (Deviation of OutLier) and REC criterion (rejection of the candidate). The details of these tests can be found in (Goda, 2010).

After the best fitting distribution is determined, the extreme value corresponding to any return period Rp (in years) is calculated with the inverse function of cumulative distribution as:

$$x_{Rp} = F^{-1}(1 - \frac{1}{\lambda Rp}) \tag{6}$$

where; λ is the mean rate or the number of sample data per year.

### 5.1. Extreme value analysis for the wind speed

The result of extreme wind speed analysis is given by plotting the non-exceedance probability, $P(<u_{10})$ versus wind speed for the Gumbel distribution, which is the best fitting one. It is demonstrated in Fig. 17 together with the return periods of 10, 30, 50 and 100 years on the upper -× axis. As can be seen in Fig. 17, the wind speed is equal to 22.486 m/s and 23.896 m/s for Rp = 50 and 100 years, respectively.

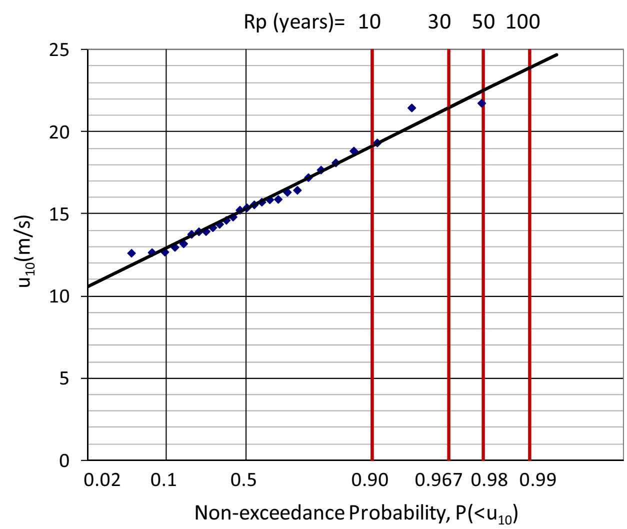


Fig. 17. Extreme wind speed (u10) statistical analysis result of the combined altimeter data.

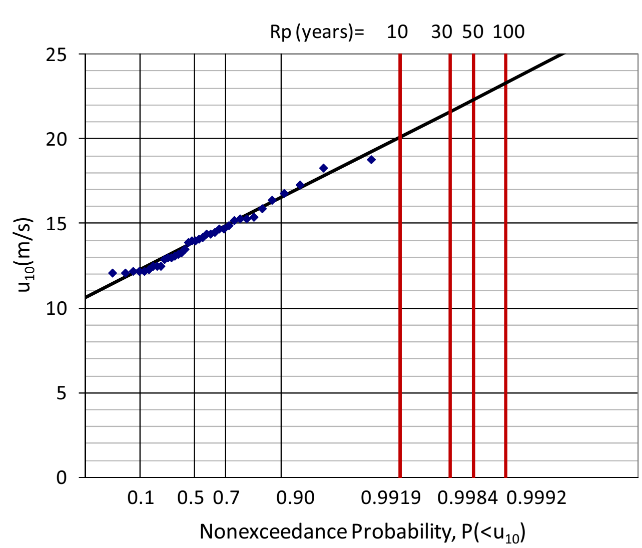


Fig. 18. Statistical analysis of extreme wind speed (u10) measured in Silivri station.

Extreme wind speeds corresponding to various return periods are also calculated from in-situ measurements in Silivri and Adalar stations. Since there are nearly three years of measurement in Silivri and 3.5 years of measurement in Adalar stations, POT method is used. Threshold wind speed value is kept as 12 m/s after some trials to get the sufficient number of data, and it is found that there are 37 independent storms with a peak wind speed higher than 12 m/s measured

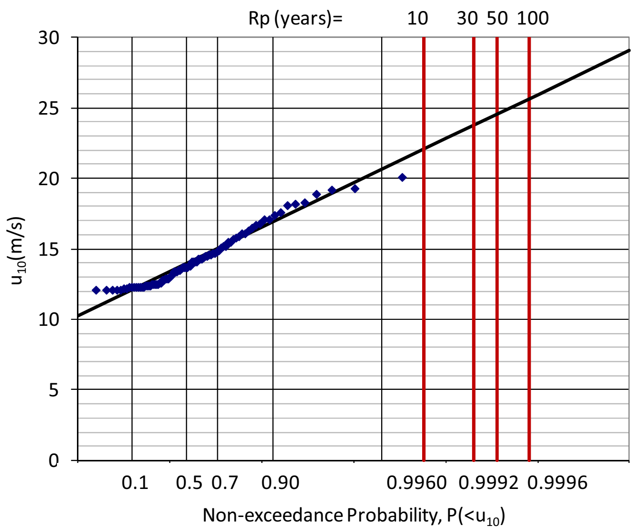


Fig. 19. Statistical analysis of extreme wind speed (u10) measured in Adalar station.

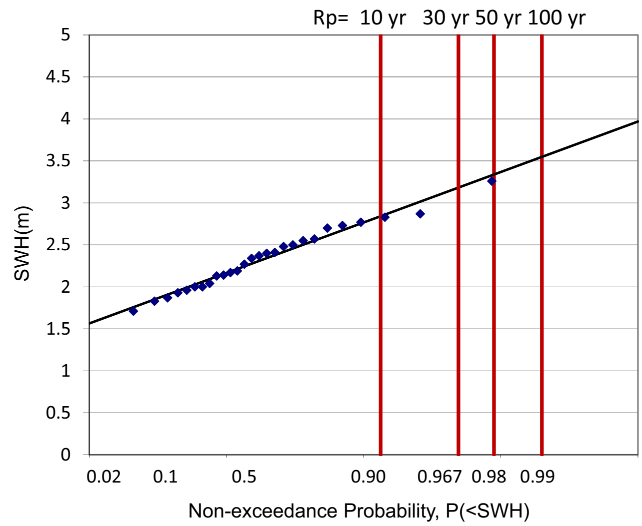


Fig. 21. Extreme value statistical analysis result for SWH of the combined altimeter data.

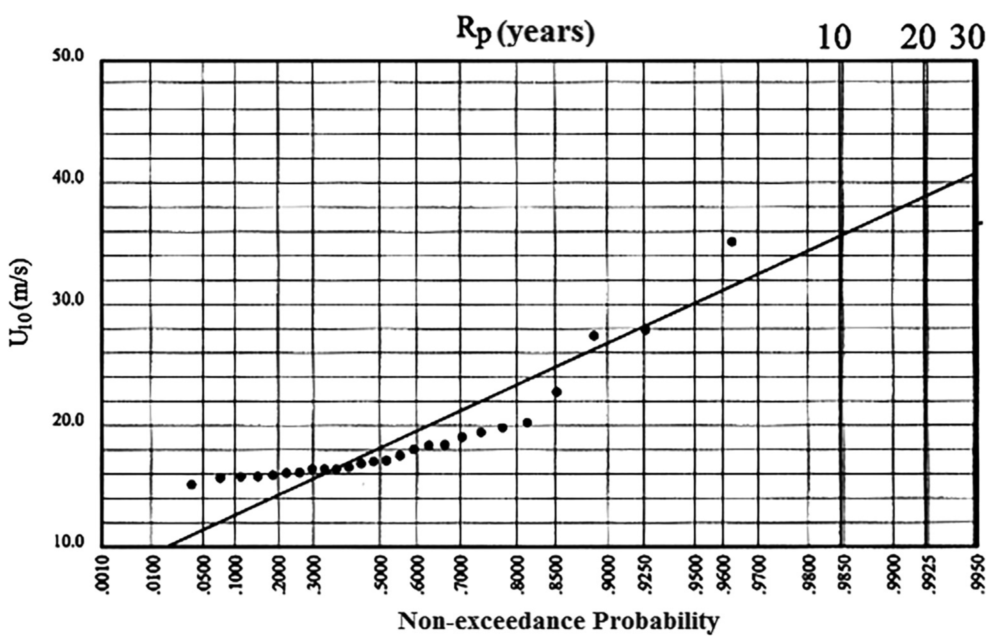


Fig. 20. Extreme wind speed analysis result of the Atlas (Ozhan and Abdalla, 2002) (Re-printed from Wind and Deep Water Wave Atlas).

Table 7
Comparison of the extreme $u_{10}$ (m/s) results corresponding to Rp = 30, 50 and 100 years.

| | Coordinate | Rp (years) 30 | 50 | 100 |
|---|---|---|---|---|
| Current study | 40.6–40.9 N 27.8–28.8 E | 21.441 | 22.486 | 23.896 |
| Atlas (Ozhan and Abdalla, 2002) | 40.98 N 28.21E | 40.000 | | |
| Measurement in Silivri | 40.97 N 28.25E | 21.637 | 22.349 | 23.315 |
| Measurement in Adalar | 40.93 N 28.95E | 24.017 | 24.820 | 25.910 |

in Silivri Station. It is 87 in case of Adalar station. Analysis for extreme value statistics is performed as explained in Section 5. The data are fitted to the Gumbel distribution. The results are shown in Fig. 18 and Fig. 19 for Silivri and Adalar stations. To calculate the extreme wind speeds with various return periods, Eq. (6) is used. Mean rate λis 37/3 for Silivri and 87/3.5 for Adalar station.

Extreme value analysis result of Wind and Deep Water Wave Atlas along the Turkish Coasts (Ozhan and Abdalla, 2002) is also given for comparison in Fig. 20. In Atlas, extreme analysis was performed with POT values among four years of data for the Marmara Sea, due to lack of sufficient data before the year of 2000. Therefore return value could not be given beyond 30 years return period due to reliability concerns. While the wind speed corresponding to 30 years return period is found as 21.337 m/s in the current study, it is almost 40 m/s in the Atlas.

The summary of comparison results are given in Table 7.

Table 7 indicates that extreme wind speed results of the current study corresponding to 30, 50 and 100 years return period are very similar to the results of the Silivri buoy. Extreme values computed using wind speed data of Adalar station are higher than those of Silivri and the current study. It may be due the fact that the matchup area is more representative to compare RA data with the measurements in Silivri buoy rather than Adalar station.

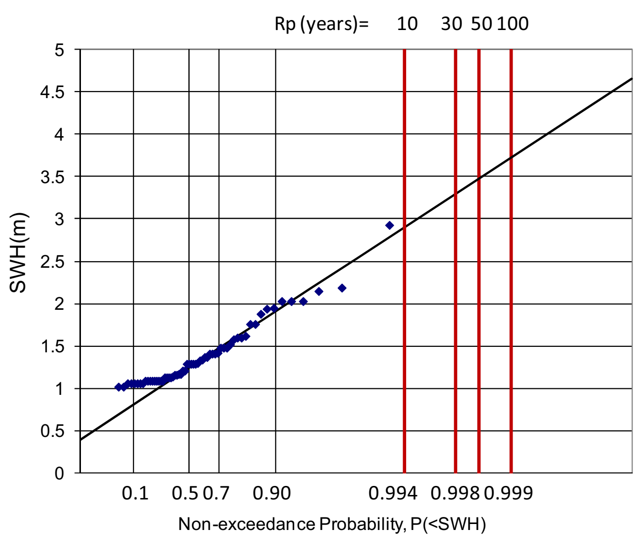


Fig. 22. Extreme value statistical analysis result for SWH of the Silivri buoy.

### 5.2. Extreme value analysis for the significant wave height (SWH)

An extreme value analysis similar to that in Section 5.1 is performed for SWH. Annual maxima of 27 years calibrated radar altimeter SWH data are used. They are arranged in descending order, and non-exceedance probabilities are calculated with the plotting position formula given in Eq. (1). Then the probabilities are fit to a theoretical distribution function by the least squares method. Finally, the goodness of fit is tested. Test results show that the Gumbel distribution is the best fitting one. The result of extreme SWH analysis is given by plotting the non-exceedance probability, P(x) versus SWH for the Gumbel distribution. This is shown in Fig. 21. The significant wave heights corresponding to return periods of 10, 30, 50 and 100 years can easily be found in Fig. 21. As can be seen in Fig. 21, the SWH is equal to 3.338 m and 3.548 m for Rp = 50 and 100 years, respectively.

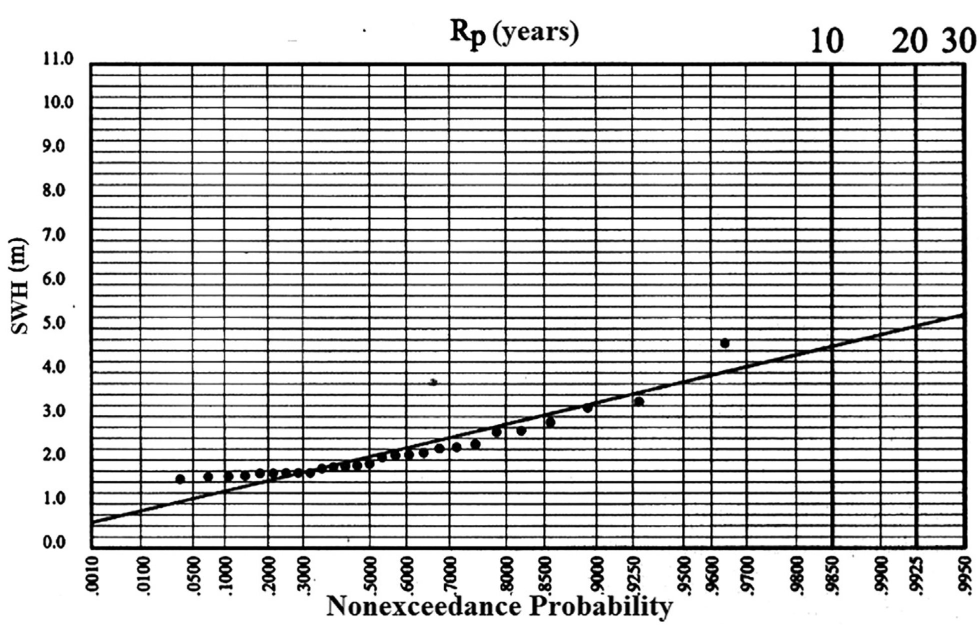


Fig. 23. Extreme SWH analysis result of the Atlas (Ozhan and Abdalla, 2002) (Re-printed from Wind and Deep Water Wave Atlas, for 40.980N, 28.210E).

Extreme SWH corresponding to various return periods are also calculated from buoy measurements in Silivri station. Since the total measurement duration in Silivri station is nearly four years, POT method is used to compute extreme SWH. Threshold SWH value is kept as 1.0 m after some trials to get the sufficient number of data, and it is found that there are 63 independent storms with a peak SWH higher than 1.0 m measured in Silivri station. Analysis for extreme value statistics is performed as explained in Section 5. Gumbel distribution is fitted to the data. The result is shown in Fig. 22. In order to calculate the extreme SWH corresponding to various return periods, Eq. (6) is used. Mean rate l is 63/4 for Silivri buoy measurements.

Extreme SWH analysis results of the current study are also compared with the results of the previous studies. Extreme SWH analysis result of Wind and Deep Water Wave Atlas (Ozhan and Abdalla, 2002) is given in Fig. 23 for 40.98$^0$N, 28.21$^0$E which is the nearest point to the buoy location.

Saracoğlu (2011) obtained deep water wave climate for the Marmara Sea using the wind fields from ECMWF and the 3rd generation wave model Mike 21 SW. His extreme SWH analysis result is shown for 40.98$^0$N, 28.21$^0$E in Fig. 24.

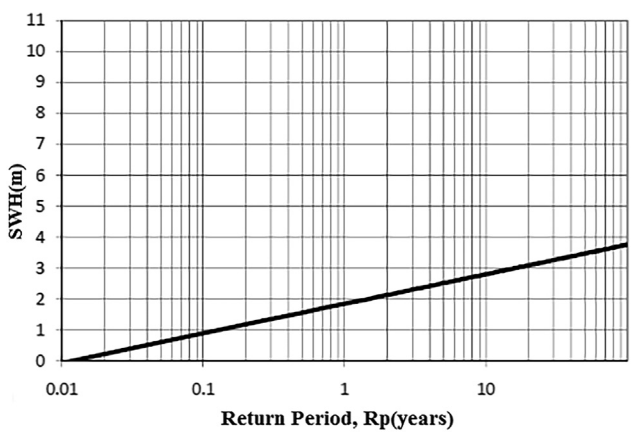


Fig. 24. Extreme SWH analysis result of Saracoğlu (2011) (Re-printed).

Kutupoglu et al. (2018) also estimated the extreme SWH with various return periods for the Marmara Sea. They used maximum values of monthly significant wave heights for the year 2013 from both their SWAN simulations and the buoy measurements of Silivri in their extreme statistics analysis. The data were fitted to the Gumbel distribution and their statistical results of extreme values are given in Fig. 25.

In Fig. 25, the x-axis represents the value of the inverse function of the Gumbel distribution. The upper line of the x-axis represents the annual return period, Rp. However, it seems that the correspondence between the return period and the value of the inverse function of the Gumbel distribution in Fig. 25 is not correct. If Rp = 100 years, then non-exceedance probability P(<Hm0)=(1–1/(12*100)) = 0.99917 as given in Eq. (6) and –ln(-ln(P(<Hm0))) = 7.09. In Fig. 25, Rp = 100 years corresponds to –ln(-ln (P(<Hm0))) = 4.6. The difference comes from the mean rate or, in other words, the number of events per year as defined in Eq. (6). The mean rate should be equal to 12 in their study, since they used the monthly maximum SWH. However, this makes the SWH corresponding to the return period of 100 years 4.1 m rather than 3.0 m as given in Fig. 25. Therefore, the extreme SWH values in Kutupoglu et al. (2018) may be re-calculated considering that the number of events per year is 12 in the computation of non-exceedance probabilities of SWH.

The summary of comparison results are given in Table 8. The values in the parenthesis are re-calculated extreme values for Kutupoglu et al. (2018) based on Fig. 25.

Table 8 indicates that the extreme values for the SWH of the current study agrees well with those of Silivri buoy, Saracoğlu (2011) and the re-calculated values of Kutupoglu et al. (2018).

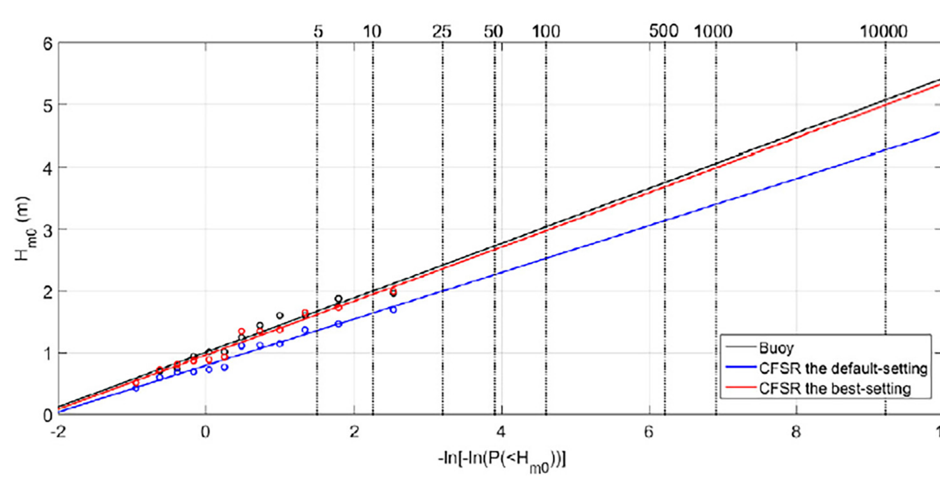


Fig. 25. Extreme wave heights with different return periods constructed based on monthly maximum significant wave heights from the calibrated and default setting SWAN models forced with the CFSR winds versus the measurements for 2013 at Silivri station (Kutupoglu et al., 2018, Re-printed).

Table 8
Comparison of the extreme SWH analysis results of the current study, measurement in Silivri and the previous studies.

| | Coordinate | Rp (years) 30 | 50 | 100 |
|---|---|---|---|---|
| Current study | 40.6–40.9N 27.8–28.8 E | 3.18 | 3.34 | 3.55 |
| Measurement in Silivri | 40.97N 28.25E | 3.01 | 3.16 | 3.36 |
| Atlas (Ozhan and Abdalla, 2002) | 40.98N, 28.21E | 5.25 | | |
| Saracoğlu (2011) | 40.98N, 28.21E | 3.2 | 3.5 | 3.8 |
| Kutupoglu et al. (2018) | 40.97N 28.25E | 2.4 (3.5) | 2.67 (3.7) | 2.98 (4.1) |

## 6. Conclusions

In this study, for the first time, the altimeter wind speed and significant wave height data from different satellite missions are attempted to use in the extreme value analysis of the Marmara Sea, an inland sea within the boundaries of Turkey.

The altimeter wind speed of Jason2, Saral, CryoSat2, Jason3 and Sentinel3 are individually compared with the Silivri buoy and Adalar station data for the period 2013–2018. In order to increase the collocation number, all the altimeter data (Jason2, CryoSat2, Saral, Jason3, Sentinel3) are combined and one satellite database is obtained for the comparison with the in-situ measurements. While the individual altimeters underestimate or overestimate the probability of high wind speeds, the combined altimeters result in a good agreement with the in-situ measurements.

A similar comparison study was carried out for the significant wave height (SWH). Comparison plots of Silivri buoy SWH versus individual satellites and the combination of them show that the agreement between RA data and the buoy data is not sufficiently good. Altimeters measure higher SWH compared to the Silivri buoy. Therefore it is decided to calibrate the SWH data measured by altimeters.

The recent altimeter data used in the comparison study are combined with the earlier satellite data to extend the duration of the continuous altimeter time record to more than two decades. An inter-calibration exercise is done for Jason2, Jason1 and Topex. As a result, 27 years long wind speed and SWH data are obtained to use in the extreme value statistics.

As a result of extreme value statistical analysis, the extreme wind speed and the significant wave height values corresponding to various return periods are determined and compared with the in-situ measurements and the results of previous studies. For both wind speed and SWH, extreme values of the current study are less than the Atlas (Ozhan and Abdalla, 2002). However, they are consistent with the extreme value results of the in-situ measurements. SWH results also agree well to model data results of Saracoğlu (2011) and the re-calculated values of Kutupoglu et al. (2018). Consistent extreme values computed during the current study result in the conclusion that the combined radar altimeter data can be used in wind and wave climate calculations and extreme value analysis of the Marmara Sea after necessary calibrations.

## Acknowledgements

I would like to thank TSMS (Turkish State Meteorological Service) for providing the in-situ measurement data at Silivri and Adalar.

This work was supported by Turkish Research Council, TUBITAK under the Grant: 117M968.

## References

Abdalla, S., 2013. Wind and wave data selection for climate studies in enclosed seas. In: Proceedings of the global congress on integrated coastal management: lessons learned to address new challenges EMECS 10 - MEDCOAST 2013, E. Özhan (Editor), 30 October - 3 November 2013, Marmaris, Turkey, pp. 1347–1358.

Abdalla, S., Ozhan, E., Erkal, S., 1998. Wind and wave climate of the Sea of Marmara. Ocean Wave Measur. Anal. 1 (2), 1282–1294.

Abdalla, S., Ozhan, E., 1999. Wind and Wave Atlas of the Black Sea. In: Proceedings of the MEDCOAST 99- EMECS 99 joint conference: land ocean interactions-managing coastal ecosystems, 9-13 November 1999, Antalya, Vol. 3. pp. 1767–1781.

Abdalla, S., Janssen, P.A.E.M., Bidlot, J.R., 2011. Altimeter near real time wind and wave products: Random error estimation. Mar. Geod. 34 (3–4), 393–406.

Abdalla, S., Yılmaz, N., 2015. Suitability of ECMWF ERA-20C for Wind and Wave Climate in the Black Sea. In: Proceedings of the twelfth international conference on the mediterranean coastal environment MEDCOAST 2015, 6-10 October 2015, Varna, Bulgaria, pp. 745–755.

Abdollahzadehmoradi, Y., Erdik, T., Özger, M., Altunkaynak, A., 2014. Application of MIKE 21 SW for wave hind casting in Marmara sea basin for the year 2012. In: Proceedings of 11th international congress on advances in civil engineering. ACE, İstanbul, Turkey. pp. 21–25.

Erkal, S., 1997. Wind Climate of the Sea of Marmara Based on a Wind Model. Master Thesis. Middle East Technical University, Ankara.

Goda, Y., 2010. Random seas and design of maritime structures. Advanced series on ocean engineering: Vol. 33, 3rd ed. World Scientific Publishing Co. Pte. Ltd., Singapore.

Hithin, N.K., Kumar, V.S., Shanas, P.R., 2015. Trends of wave height and period in the Central Arabian Sea from 1996 to 2012: A study based on satellite altimeter data. Ocean Eng. 108, 416–425.

Janssen, P.A.E.M., Abdalla, S., Hersbach, H., Bidlot, J.-R., 2007. Error estimation of buoy, satellite, and model wave height data. J. Atmos. Oceanic Technol. 24, 1665–1677.

Kamphuis, J.W., 2000. Introduction to coastal engineering and management. Advanced Series on Ocean Engineering: Vol. 30, 1st ed. World Scientific Publishing Co. Pte. Ltd., Singapore.

Kutupoglu, V., Cakmak, R.E., Akpinar, A., 2018. Setup and evaluation of a SWAN wind wave model for the Sea of Marmara. Ocean Eng. 165, 450–464.

Ministry of Transport, 2010. Master Plan Study for the Turkish Ports and Harbors. Final Report by Yuksel Project Comp. Ankara.

ONHO, 2015. Catalog of Offshore Buoys. Turkish Naval Forces Command Office of Navigation, Hydrography and Oceanography.

Ozhan, E., Abdalla, S., 1999. Wind and wave Climotology of Turkish Coasts and The Black Sea: An Overview of the NATO TU_WAVES Project. In: Proceeding of MEDCOAST Conference on Wind and Wave Climate of the Mediterranean and the Black Sea, Antalya-Turkey, pp. 1–20.

Ozhan, E., Abdalla, S., 2002. Wind and Deep Water Wave Atlas along the Turkish Coasts. MEDCOAST, ODTU, Ankara, 445 pages (in Turkish).

Saracoğlu, E.K., 2011. The Wave Modelling and Analysis of the Black Sea and the Sea of Marmara. Master Thesis. Institute of Science and Technology, Yıldız Technical University, Turkey (in Turkish).

Scharroo, R., Leuliette, E.W., Lillibridge, J.L., Byrne, D., Naeije, M.C., Mitchum, G.T., 2013. RADS: Consistent multi-mission products. In: Proc. of the Symposium on 20 Years of Progress in Radar Altimetry, Venice, 20-28 September 2012, Eur. Space Agency Spec. Publ., ESA SP-710, p. 4 pp.

Vinoth, J., Young, I.R., 2011. Global estimates of extreme wind speed and wave height. J. Climate 24 (6), 1647–1665.

Young, I.R., Zieger, S., Babanin, A., 2011. Global trends in wind speed and wave height. Science 332 (6028), 451–455.

Zieger, S., Vinoth, J., Young, I.R., 2009. Joint calibration of multiplatform altimeter measurements of winds peed and wave height over the past 20years. J. Atmos. Ocean. Technol. 26, 2549–2564. https://doi.org/10.1175/2009JTECHA1303.1.